Research Article

Jianwei Wang, Kun Wang, Tianling Qin*, Hanjiang Nie, Zhenyu Lv, Fang Liu, Xiaoqing Shi, and Yong Hu

Analysis and prediction of LUCC change in Huang-Huai-Hai river basin

https://doi.org/10.1515/geo-2020-0112
received March 28, 2020; accepted October 29, 2020

Abstract: Land use/cover change plays an important role in human development and environmental health and stability. Markov chain and a future land use simulation model were used to predict future change and simulate the spatial distribution of land use in the Huang-Huai-Hai river basin. The results show that cultivated land and grassland are the main land-use types in the basin, accounting for about 40% and 30%, respectively. The area of cultivated land decreased and artificial surfaces increased from 1980 to 2010. The degree of dynamic change of land use after the 1990s was greater than that before the 1990s. There is a high probability of exchange among cultivate land, forest and grassland. The area of forest decreased before 2000 and increased after 2000. Under the three emission scenarios (RCP2.6, RCP4.5, and RCP8.5) of IPSL-CM5A-LR climate model, the area of cultivated land will decrease and that of grassland will increase in the upstream area while it will decrease in the downstream area. The above methods and rules will be of great help to future land use planning.

Keywords: LUCC, marcochains, FLUS, climate change, Huang-Huai-Hai river basin

1 Introduction

Land use and land cover change (LUCC) research plays an important part in the global change research [1–3]. Human alterations in land cover as a result of the use of land-based natural resources not only have local and regional impacts but can also have important effects at the global level [4]. Under the adjustment of institutional factors, people's response to economic opportunities promoted changes in land cover [5]. Inundation and resettlement will cause LUCC [6]. Economic, technological, institutional, and location factors are often considered as potential drivers of LUCC [7]. The accelerated industrialization and urbanization following economic reforms and population increases have greatly affected LUCC through the increase of built-up areas and urban sprawl [8]. The fragmentation of cultivated land can be observed due to construction on the land of the countryside [9]. In addition to human activities, climate change also affects LUCC [10]. Climate change will cause changes in temperature and precipitation, affecting vegetation growth and the temporal and spatial distribution of water resources. Grasslands are most responsive to extreme drought events followed by forests and desert vegetation [11]. After experiencing 8 years of extreme drought events in the San Juan National Forest, Colorado, USA, the average dieback rate of Populus tremuloide gradually increased from 15% to 27% in July 2011 and to 38% in July 2012 [12]. In the long-term, repeated drought-induced mortality events, along with unsuccessful recruitment of the dominant tree species in forests may lead to a vegetation succession process where trees would be replaced by understory species (such as drought-tolerant shrub) [13]. Comprehensively consider the impact of human activities and climate

* **Corresponding author: Tianling Qin,** State Key Laboratory of Simulation and Regulation of Water Cycle in River Basin, China Institute of Water Resources and Hydropower Research, Beijing, China, e-mail: qintl@iwhr.com
Jianwei Wang, Kun Wang: State Key Laboratory of Simulation and Regulation of Water Cycle in River Basin, China Institute of Water Resources and Hydropower Research, Beijing, China
Hanjiang Nie, Zhenyu Lv, Xiaoqing Shi: State Key Laboratory of Simulation and Regulation of Water Cycle in River Basin, China Institute of Water Resources and Hydropower Research, Beijing, China, Department of Hydraulic Engineering, Tsinghua University, Beijing, China
Fang Liu: College of Environmental Science and Engineering, Donghua University, Shanghai, China
Yong Hu: State Key Laboratory of Simulation and Regulation of Water Cycle in River Basin, China Institute of Water Resources and Hydropower Research, Beijing, China, Key Laboratory of Water Conservancy and Water Resources of Anhui Province, Water Resources Research Institute of Anhui Province and Huai River Water Resources Commission, MWR, Bengbu, Anhui, China

change on LUCC and predict future LUCC to provide a basis for our future land planning.

There are many methods for LUCC research. The spatial calculating analysis model is used to analyze LUCC [14]. Remote sensing and Geographic Information Systems (GIS) are also used in LUCC research [15]. Change-vector analysis is a valuable technique for LUCC detection [16]. A system dynamic model can be used to model LUCC [17]. CA (Cellular Automata)-Markov model is commonly used for LUCC prediction [18,19]. Land use simulation model Conversion of Land Use and its Effect at Small regional extent utilizes the spatial dominant dynamic simulation model established by Wageningen University [20,21]. The future land use simulation model (FLUS [The FLUS model could be downloaded from http://www.geosimulation.cn/flus.html]) developed by Liu et al. [22] could be used for multiple LUCC dynamic simulation. The FLUS model considers the impact of climate conditions, geography, and socioeconomic factors on LUCC and simulates the spatial distribution of various land-use type under different land-use conversion targets. The LUCC can provides information for our better decision on the development and utilization of natural resources [23,24]. According to research goals of this article, we choose GIS spatial analysis ang FLUS model as research tools.

The Huang-Huai-Hai river basin accounts for 15% of China's total land area. It is an important economic center and food production base in China and has an important strategic position in China's development [25]. The plains in the eastern part of the basin are China's agricultural production bases. The area of arable land and grain output account for 20.4% and 23.6% of the country's total [26]. Since the twenty-first century, the economic development of the Huang-Huai-Hai river basin has driven the process of urbanization and great changes have taken place in land-use types. The Huang-Huai-Hai region is located in China's three major climatic regions, including monsoon climate, dry climate, and highland climate. The climate change in recent years has an impact on the region, especially for the vegetation. LUCC research is of great significance to the future sustainable development of the Huang-Huai-Hai river basin. Hence, the law of LUCC and the spatial distribution of LUCC under future climate conditions will be studied in this paper.

2 Models and methods

Based on historical land use data, the Raster Calculator in the ArcGIS spatial analysis tool is used to calculate relevant indicators and transfer matrices of LUCC to analyze the laws of historical changes.

The other part is the spatial distribution of LUCC under future climate conditions. Historical land-use data, socioeconomic data, and climate data are input into the FLUS model for verification. The future climate conditions are input into the verified model to simulate the spatial distribution of LUCC under future climate conditions. The article process and structure are shown in Figure 1.

2.1 Metric indexes of LUCC

Land use of a dynamic degree is used to analyze the dynamic change of land use. The single land-use dynamic degree refers to the quantity change of a certain land-use type [27] within a certain period. The formula [28] is as follows:

$$K = \left[\frac{U_b - U_a}{U_a} \times \frac{1}{T} \times 100\% \right] \quad (1)$$

where K is the dynamic degree of one land-use type during the study period; U_a and U_b are the area of a certain land-use type at the beginning and end time of the study period, respectively; and T is the length of the study period. When T is set to the year, K is the annual change rate of a land-use type during the study period.

The comprehensive land-use dynamics degree indicates the overall dynamics of land use in a certain area. The formula [28] is as follows:

$$\mathrm{LC} = \left[\frac{\sum_{i=1}^{n} \mathrm{LC}_{i=j}}{2\sum_{i=1}^{n} \mathrm{LU}_i} \right] \times \frac{1}{T} \times 100\% \quad (2)$$

where LC is the rate of change in land use and reflects the degree of change in the amount of land use; LU_i is the area of land-use type i at the beginning of the period; LC_{i-j} is the absolute value of the area converted from land use of type i to that of non-type i during the period; and T is the length of the study period. When T is set to the year, LC is the annual change rate of a land-use type during the study period.

2.2 Markov model

The Markov model determines the changing trend of each state of the system through the initial probability of different states of the systems and the transition probability between states, to achieve the purpose of predicting the

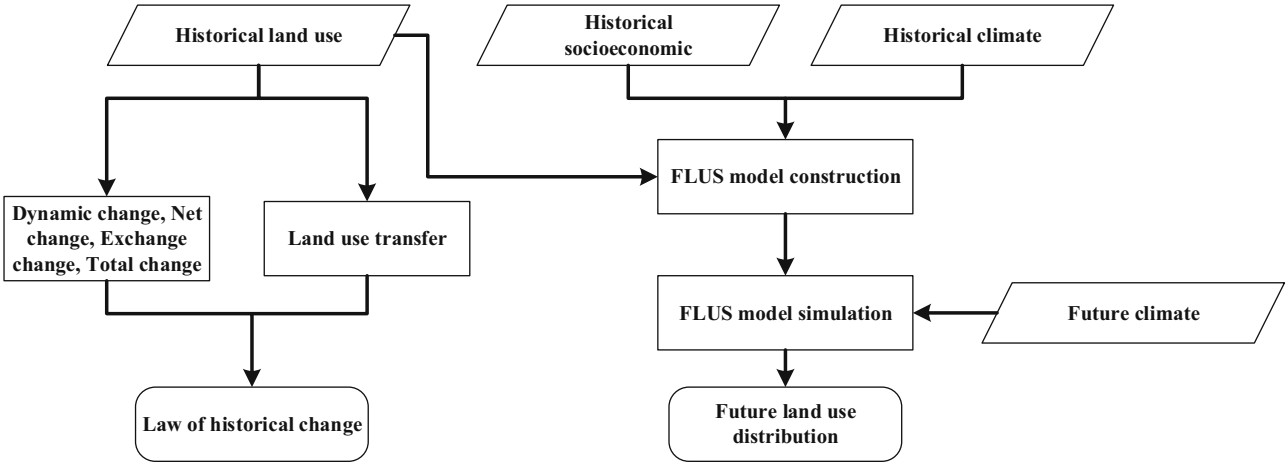

Figure 1: Article structure diagram.

future. Different land-use types in a certain area are mutually convertible, and the average conversion state change of land-use structure is relatively stable over a period of time. Therefore, the dynamic evolution of land use has the property of the Markov model. The Markov model has been widely used in the LUCC research [29]. With the support of the ArcGIS software, the land use raster of two periods are overlapped and the corresponding property in the overlay map database PAT.DBF is extracted. According to the probability distribution matrix of initial $S(0)$ and the transition probability of the nth stage $P^{(n)}$, the future area of land use could be calculated by computer simulation. The Markov simulation model $S(n)$ [30] is as follows:

$$S(n) = S(n-1) \times P^{(1)} = S(0) \times P^{(n)} \tag{3}$$

2.3 FLUS model and verification

Land-use change models are usually used to detect where the change occurred or will potentially occur [31]. Traditional methods can provide static analysis of the LUCC for the fixed beginning and end date [32]. And the LUCC model also can help people better understand the mechanism of social, economic, and physical variables' impacts on LUCC [33]. Through knowing the factors contributing to the change, the model provided a probabilistic prediction of where the change may occur [34,35]. LUCC models are also used to assess the cumulative impact of land-use change and develop future scenarios [36]. It helps and supports land-use planning and decision-making [37]. The FLUS model (Figure 2) that interactively integrates top-down system dynamics (SD) with a bottom-up CA model could be used for multiple LUCC dynamic simulation [22]. The SD model is used to project the land-use scenario demands under various socio-economic and environmental driving factors. A self-adaptive inertia and competition mechanism is developed within the CA model to process the complex competitions and interactions among the different land-use types. This model has been successfully applied in the simulation of land use and land cover change in China, as well as on the global scale [38]. In the model simulation process, not all land-use types can be transformed into each other. According to the natural evolution of land resources and the actual situation of human activities, we set up a cost matrix (Table 1). For example, artificial surface cannot be converted into other types of land, cultivated land can be converted into other types of land, and water bodies can be converted into other types of land. In this way, the simulation is more realistic.

Receiver operation characteristic (ROC) curve analysis can obtain multiple pairs of true (false) positive rate values [39]. With the false positive rate on the abscissa and the true positive rate on the ordinate, the drawn curve is called the ROC curve, and the area under the ROC curve is the AUC value (area under the curve), which reflects the value of the diagnostic test. It is generally believed that when the AUC value is 0.5–0.7, the diagnostic value is low; when the AUC value is 0.7–0.9, the diagnostic value is moderate; when it is greater than 0.9, the diagnostic value is good. Cohen's kappa coefficient [40,41] is a measure of agreement between two variables. The ROC curve and kappa are used to test the simulation effect of the FLUS model.

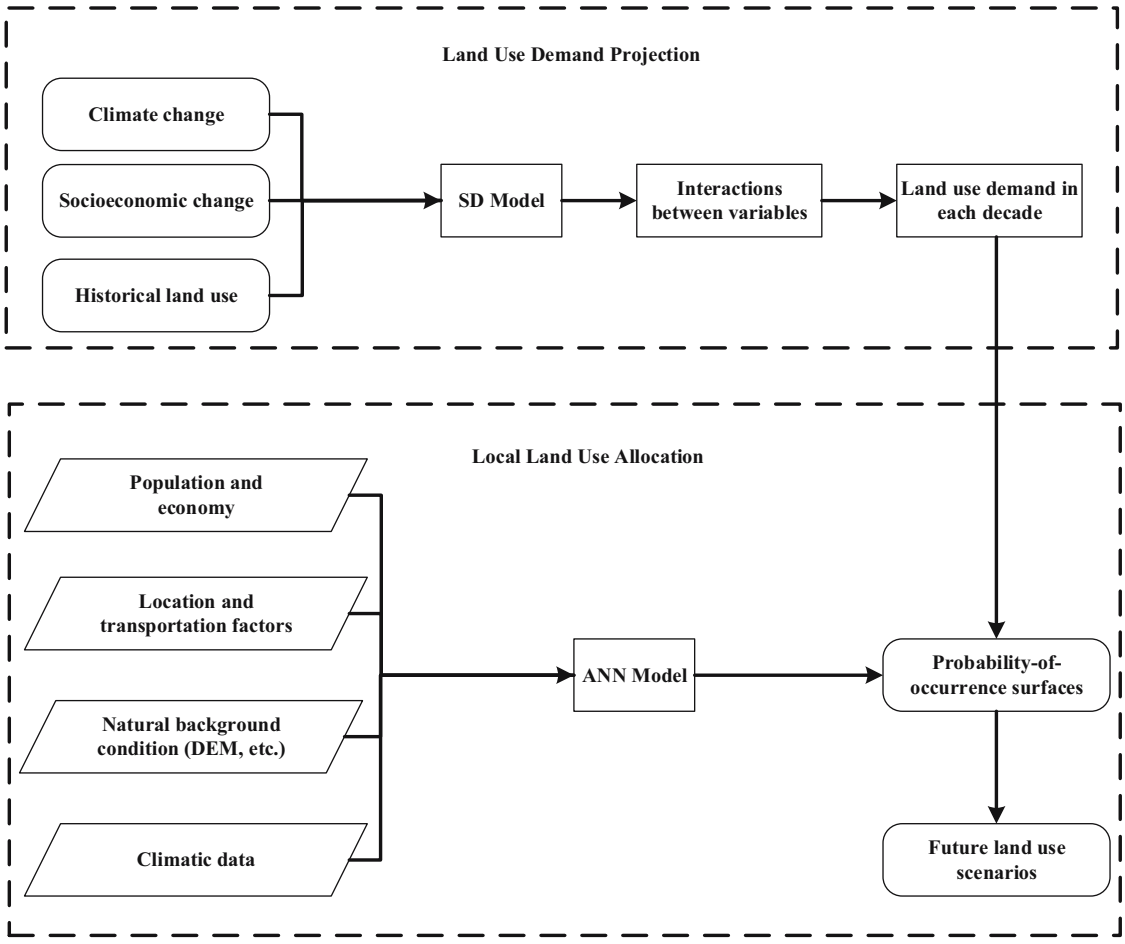

Figure 2: FLUS model frame diagram.

Table 1: Cost matrix in the FLUS model

	Cultivated land	Forest	Grassland	Water bodies	Artificial surfaces	Unutilized land
Cultivated land	1	1	1	1	1	1
Forest	1	1	0	0	1	0
Grassland	1	1	1	0	1	0
Water bodies	0	0	0	1	0	0
Artificial surfaces	0	0	0	0	1	0
Unutilized land	1	1	1	1	1	1

Note: 1 means conversion is allowed; 0 means conversion is not allowed.

3 Study area and datasets

3.1 Study area

The geographical range of the Huang-Huai-Hai area is 95°53′~122°60′E, 32°10′~43°N, with a total area of about 1.43 million km^2. The Huang-Huai-Hai region is located in China's three major climatic regions, including monsoon climate, dry climate, and highland climate. And it includes three first-level water resource regions, namely, the Yellow river basin, the Huai river basin, and the Hai river basin. The geographical location of the Huang-Huai-Hai area is shown in Figure 3.

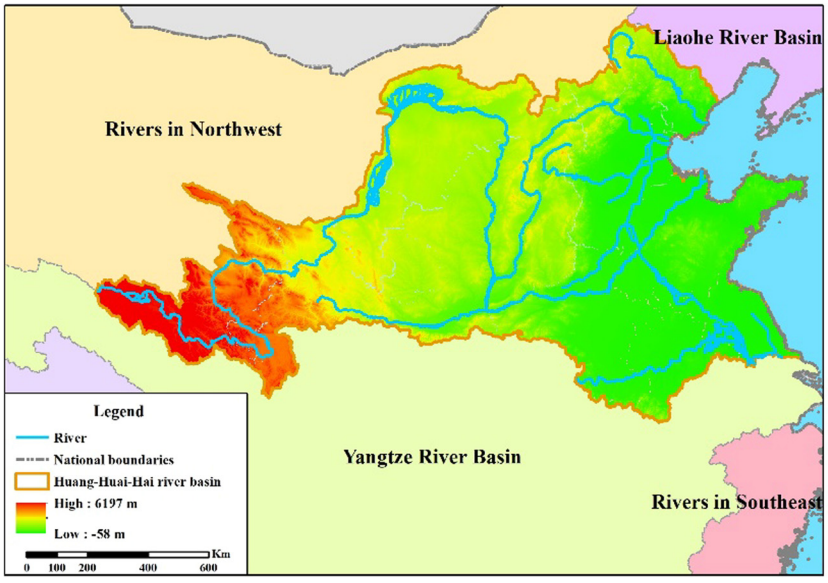

Figure 3: Location of the Huang-Huai-Hai river basin.

3.2 Data datasets

The data used in this article are land use data, socioeconomic data, terrain data, and historical climate data. The time resolution of the data is years, and the spatial resolution is 1 km × 1 km. Future climate data (liner interpolated and bias-corrected) obtained from Global Climate Model (IPSL-CM5A-LR) provided by ISI-MIP (The Inter-Sectoral Impact Model Intercomparison Project) [42]. The details are listed in Table 2.

4 Results

4.1 Law of land use conversion

4.1.1 Dynamic change of land use

Land cover proportions in the Huang-Huai-Hai river basin during 1980–2010 were calculated as listed in Table 3. The land use types in the Huang-Huai-Hai river basin were mainly composed of cultivated land, forest, and grassland in the past 20 years. And the area of the three land types accounted for more than 85% of the total area. From the perspective of the dynamics of land use change, the cultivated land has been decreasing, the artificial surfaces have been increasing, and the forest area has been reduced before increasing in the three periods (year 1980–1990, year 1990–2000, year 2000–2010). Overall, the degree land-use change after the 1990s was significantly higher than that before the 1990s.

4.1.2 Net change, exchange change, and the total change in land-use types

Based on the analysis of statistical results in Table 4, during the three periods, artificial land was dominated by expansion and cultivated land was dominated by the conversion of spatial location. Water bodies and grassland were degraded and were accompanied by some spatial conversion. In particular, the forest area increased during 2000–2010 and its net change accounted for 76% of the total change.

4.1.3 Land-use conversion

The land-use changes during 1980–2010 were analyzed from the perspective of quantitative. In order to analyze the mutual transformation of land use, the land use conversion matrix was calculated based on the ArcGIS platform. The results from 1980 to 1990 are listed in Table 5. The loss of cultivated land was mainly converted into artificial surfaces, and the degradation of water bodies was mainly converted into cultivated land. The land-use conversion results from 1990 to 2000 are listed in Table 6. The loss of cultivated land was mainly converted into artificial surfaces and also converted into water bodies and grassland. At the same time, the water bodies

Table 2: List of data used in this study

Category	Data	Year	Data resource	Description
Land use	Land use	1980\1990\2000\2010	http://www.resdc.cn	Download from the data resource and the size is 1 km × 1 km
Socioeconomic data	Population GDP	2005		
Terrain	DEM	2000	http://www.gscloud.cn	Same as above
	Aspect		—	Calculated from DEM
	Slope		—	Calculated from DEM
Roads	Road		http://www.openstreetmap.org	Convert shp file to 1 km × 1 km raster file
Climate	Temperature Precipitation	2001–2010	http://www.resdc.cn	Download from the data resource and the size is 1 km × 1 km
Future climate	Temperature	2011–2030	http://www.isi-mip.org	Resampled 0.5° × 0.5° raster into 1 km × 1 km

Table 3: Land cover proportion and dynamics in Huang-Huai-Hai river basin during 1980–2010 unit: %

Land-use type	Cover proportion					Dynamics	
	1980	1990	2000	2010	1980–1990	1990–2000	2000–2010
Cultivated land	41.97	41.94	41.79	41.10	−0.06	−0.36	−1.67
Forest	13.10	13.08	13.06	13.25	−0.15	−0.14	1.46
Grassland	31.98	31.99	31.77	31.62	0.04	−0.67	−0.49
Water bodies	2.57	2.40	2.44	2.49	−6.45	1.61	1.96
Artificial surfaces	5.17	5.39	5.83	6.40	4.11	8.31	9.66
Unutilized land	5.22	5.20	5.10	5.15	−0.29	−1.99	1.01
Total	100	100	100	100	0.35*	0.83*	0.87*

Note: * indicates a comprehensive land-use dynamics degree.

Table 4: Summary of land-use change in the Huang-Huai-Hai river basin during 1980–2010 unit: %

Statistical variables	Year range	Land-use types						Total
		Cultivated land	Forest	Grassland	Water bodies	Artificial surfaces	Unutilized land	
Increase	1980–1990	0.19	0.02	0.11	0.09	0.21	0.07	0.70
	1990–2000	0.47	0.12	0.32	0.15	0.45	0.15	1.66
	2000–2010	0.22	0.25	0.32	0.16	0.58	0.21	1.73
Loss	1980–1990	0.21	0.04	0.10	0.26	0.00	0.09	0.70
	1990–2000	0.62	0.13	0.53	0.11	0.01	0.26	1.66
	2000–2010	0.92	0.06	0.47	0.11	0.01	0.16	1.73
Net change	1980–1990	0.02	0.02	0.01	0.17	0.21	0.02	0.45
	1990–2000	0.15	0.01	0.21	0.04	0.44	0.11	0.96
	2000–2010	0.7	0.19	0.15	0.05	0.57	0.05	1.71
Exchange change	1980–1990	0.38	0.04	0.2	0.18	0	0.14	0.94
	1990–2000	0.94	0.24	0.64	0.22	0.02	0.3	2.36
	2000–2010	0.44	0.12	0.64	0.22	0.02	0.32	1.76
Total change	1980–1990	0.4	0.06	0.21	0.35	0.21	0.16	1.39
	1990–2000	1.09	0.25	0.85	0.26	0.46	0.41	3.32
	2000–2010	1.14	0.31	0.79	0.27	0.59	0.37	3.47

Table 5: The conversion matrix of land use from 1980 to 1990

Year 1980 (km^2)	Year 1990 (km^2)						
	Cultivated land	Forest	Grassland	Water bodies	Artificial surfaces	Unutilized land	Total
Cultivated land	6,00,639	108	88	851	1,966	49	6,03,701
Forest	115	1,87,778	447	9	22	1	1,88,372
Grassland	635	120	4,58,538	224	167	274	4,59,958
Water bodies	1,537	48	746	33,246	656	734	36,967
Artificial surfaces	18	0	3	2	74,382	0	74,405
Unutilized land	407	37	309	250	273	73,810	75,086
Total	6,03,351	1,88,091	4,60,131	34,582	77,466	74,868	

Table 6: The conversion matrix of land use from 1990 to 2000

Year 1990 (km^2)	Year 2000 (km^2)						
	Cultivated land	Forest	Grassland	Water bodies	Artificial surfaces	Unutilized land	Total
Cultivated land	5,94,420	451	1,202	1,022	5,882	374	6,03,351
Forest	635	1,86,159	1,122	28	92	55	1,88,091
Grassland	4,250	1,032	4,52,466	393	330	1,660	4,60,131
Water bodies	1,145	52	182	33,032	55	116	34,582
Artificial surfaces	59	2	2	13	77,390	0	77,466
Unutilized land	700	123	2,069	650	153	71,173	74,868
Total	6,01,209	1,87,819	4,57,043	35,138	83,902	73,378	

and grassland were mainly converted into cultivated land. The land-use conversion results from 2000 to 2010 are listed in Table 7. The law of cultivated land conversion was still the same, but the change of forest was more obvious than the previous two periods.

4.2 Prediction and spatial distribution simulation of land-use change

4.2.1 Prediction of land-use change

The prediction steps are as follows: the first step is the generation of the initial state matrix. Select the land use types in 2000 as the initial matrix as follows (unit: km^2).

$$S(0) = [\text{Cultivated land forest Grassland waterbodies artificial surfaces untilized land}] = [6{,}01{,}209 \quad 1{,}87{,}819 \quad 4{,}57{,}043 \quad 35{,}138 \quad 83{,}092 \quad 73{,}378] \tag{4}$$

The land-use type area transition matrix of the initial state (Table 6) was obtained from 2000 to 2010. Thus, the initial state transition probability matrix (unit: %) from 2000 to 2010 (Table 8) and the annual average transition probability matrix were calculated to predict the land-use areas in 2030.

The future land-use area of change trend was calculated with the formula (3), formula (4), and Table 7. The results of 2,030 are listed in Table 9.

4.2.2 Spatial distribution simulation of land-use change

4.2.2.1 Model establishment and verification

Based on the land use of 2000, the geographical and socio-economic factors are considered to simulate the land use distribution in 2010 with the FLUS model. And the result was verified with actual data of 2010.

The simulation result of spatial land use and the actual one of 2010 are shown in Figure 4, with three small regions to display more details of the simulated results. The figure shows that the simulated pattern is well correlated with the actual. To quantitatively validate the simulated result, the confusion matrix of simulated results and the actual land use was calculated (Table 10). Then, the overall accuracy and Cohen's Kappa coefficient for all land-use types were calculated. In addition, ROC curves of different

Table 7: The conversion matrix of land use from 2000 to 2010

Year 2000 (km^2)	Year 2010 (km^2)						
	Cultivated land	Forest	Grassland	Water bodies	Artificial surfaces	Unutilized land	Total
Cultivated land	5,87,977	1,808	2,747	1,465	6,859	353	6,01,209
Forest	122	1,86,935	312	101	298	51	1,87,819
Grassland	1,754	1,633	4,50,272	454	631	2,299	4,57,043
Water bodies	761	60	225	33,520	288	284	35,138
Artificial surfaces	68	18	45	55	83,708	8	83,902
Unutilized land	479	107	1,213	231	227	71,121	73,378
Total	5,91,161	1,90,561	4,54,814	35,826	92,011	74,116	

Table 8: The initial state transition probability matrix from 2000 to 2010 ($n = 0$)

2000	2010					
	Cultivated land	Forest	Grassland	Water bodies	Artificial surfaces	Unutilized land
Cultivated land	97.80	0.30	0.46	0.24	1.14	0.06
Forest	0.06	99.53	0.17	0.05	0.16	0.03
Grassland	0.38	0.36	98.52	0.10	0.14	0.50
Water bodies	2.17	0.17	0.64	95.40	0.82	0.81
Artificial surfaces	0.08	0.02	0.05	0.07	99.77	0.01
Unutilized land	0.65	0.15	1.65	0.31	0.31	96.92

Table 9: Land use prediction results in 2030

Year	Area (km^2)					
	Cultivated land	Forest	Grassland	Water bodies	Artificial surfaces	Unutilized land
2030	5,71,780	1,95,905	4,50,394	37,057	1,07,859	75,495

land-use types in the simulation results were drawn, as shown in Figure 5. The results showed that, except for the poor simulation of unutilized land, the simulation results of the other five types were very good. Therefore, the model can be used for later predation.

4.2.2.2 Prediction of land use in future climate scenarios

Based on the previous step, the result of Markov's prediction was used as the target for future land use and was as the input into the model. IPSL-CM5A-LR is comparatively better among all five climate models in this study area [41]. The spatial distribution of land use in 2030 was simulated under different climate scenarios (RCP2.6, RCP4.5, and RCP8.5). RCP2.6, RCP4.5, and RCP8.5 represent three scenarios of low, medium, and high greenhouse gas emissions, respectively, and represent possible future climate changes. The analysis under the conditions of the three climatic models makes our research on land-use changes under the future climatic conditions more comprehensive. The results are shown in Figure 6.

According to the prediction results shown in Table 9, the area of cultivated land will decrease largely in 2030 and that of the artificial surface will increase correspondingly. Based on the prediction results of 2030, the spatial distribution of different land-use types in three different scenarios is shown in Figure 4. In the three scenarios, the spatial distribution of artificial surfaces and water bodies are the same. However, there are some differences in the spatial distribution of cultivated land, grassland, and forest. Huang-Huai-Hai river basin includes three first-level sub-watershed (Figure 7) and seventeen second-level sub-watershed (Figure 8). The areas with a great difference in the spatial distribution of land use are shown in Figure 9. The specific results are shown in Figure 10 and the meaning of basin number is listed in Table 11.

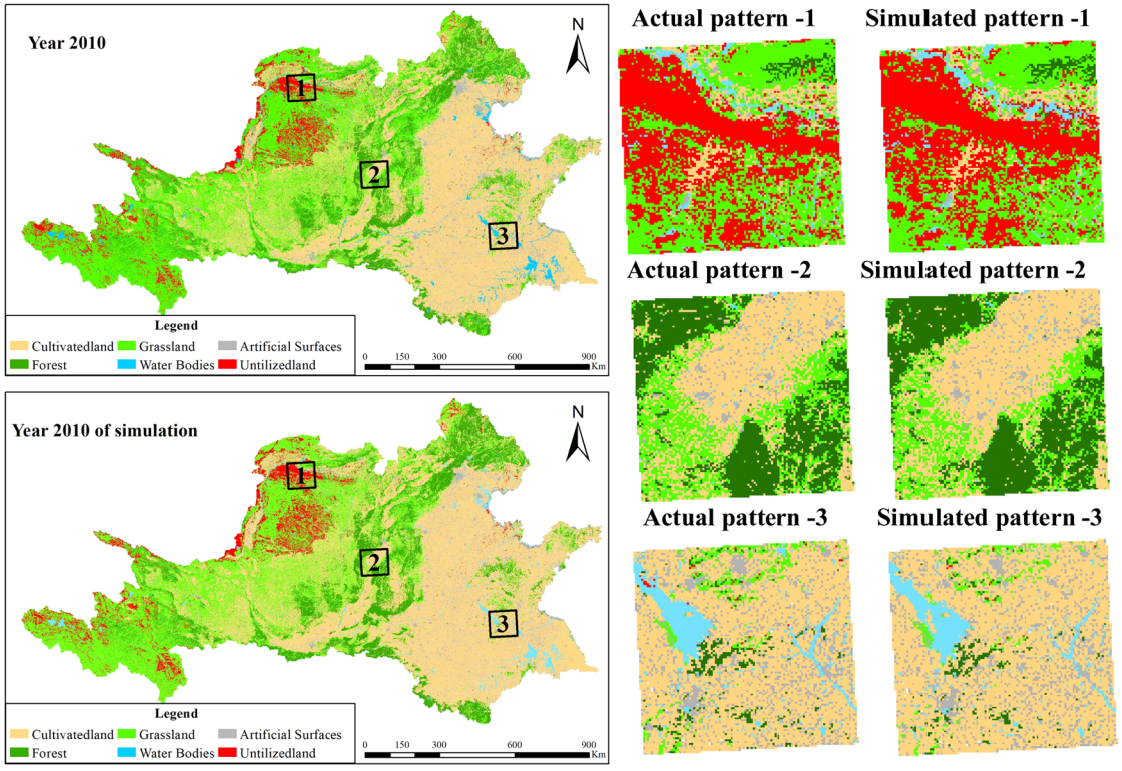

Figure 4: The simulated land-use pattern and the actual land-use pattern in 2010.

Table 10: Confusion matrix of the predicted land-use pattern versus the actual pattern in 2010

Land use types	Actual land use in 2010						Total
	Cultivated land	Forest	Grassland	Water bodies	Artificial surfaces	Unutilized land	
Cultivated land	55,875	804	882	607	649	132	58,949
Forest	762	17,398	710	46	33	22	18,971
Grassland	906	623	43,736	89	60	492	45,906
Water bodies	713	47	43	2,714	24	45	3,586
Artificial surfaces	656	26	44	32	8,269	6	9,033
Unutilized land	48	9	436	122	17	6,771	7,403
Total	58,960	18,907	45,851	3,610	9,052	7,468	1,43,848

Note: Kappa coefficient = 0.91, overall accuracy = 0.93.

5 Discussion

5.1 Impact of historical climate and human activities on land use/cover

The comprehensive land-use dynamics degree of the 1980s, 1990s, and 2000s were 0.35, 0.83, and 0.87, respectively, as shown in Table 2. After the 1990s, under the influence of Economic Reform and open up, China's economy developed rapidly. The transformation of the land by humans was huge. In particular, the acceleration of urbanization and rapid population growth have turned cultivated land, woodland, and grassland into resident land, and the water area had degraded. From a climate perspective, the temperature has increased by 1°C (1980–2010), and the increase in temperature is helpful for vegetation growth (photosynthesis) [42]. But the total amount of vegetation was still decreased. There may be two reasons for this. In the 1990s, people only paid attention to economic development and neglected the protection of vegetation. During this period, forest land and grassland decreased. In the twenty-first century, our country not only pays attention to social development but also pays attention to the protection of vegetation. Therefore, during the period from 2000 to 2010,

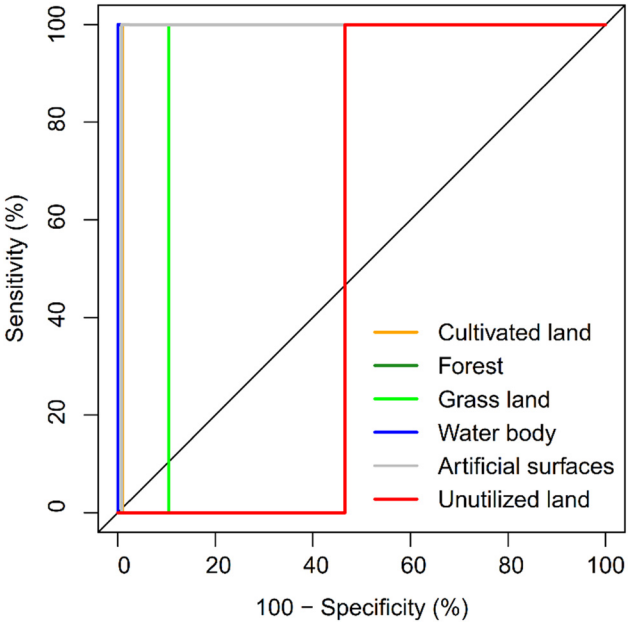

Figure 5: ROC curves of different land-use types based on simulation results in 2010.

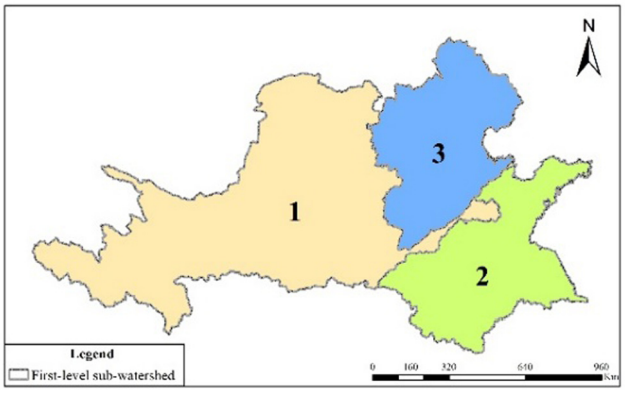

Figure 7: First-level sub-watershed.

vegetation was partially restored. The other is precipitation. Since 1980, the total amount of precipitation has not changed dramatically, but the temporal and spatial distribution of precipitation has been quite different. Especially after the 1990s, the occurrence of extreme hydrological events (droughts, floods) had an impact on the change of land cover [43,44]. The survival rate of trees is affected by extreme floods and the closer to the river,

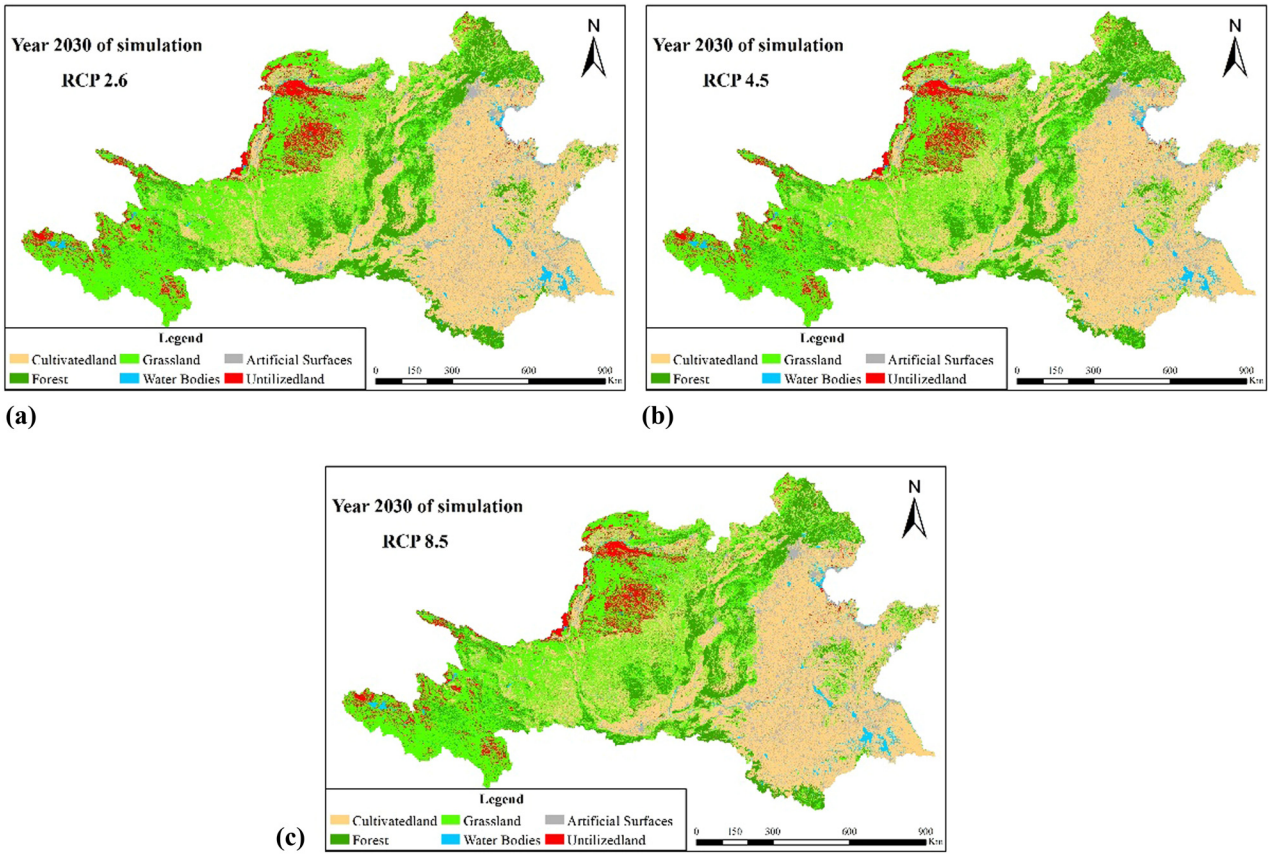

Figure 6: (a) Simulation result under RCP2.6, (b) simulation result under RCP4.5, and (c) simulation result under RCP8.5.

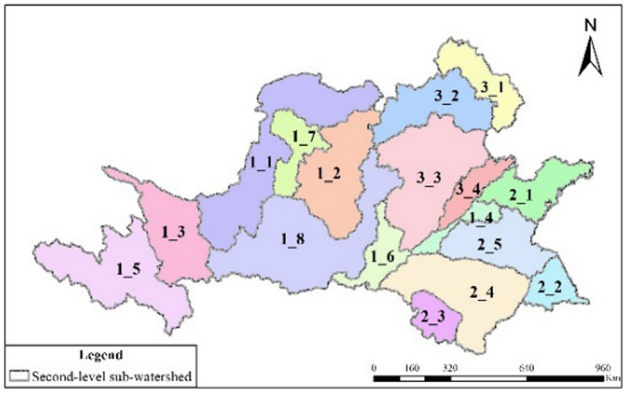

Figure 8: Second-level sub-watershed.

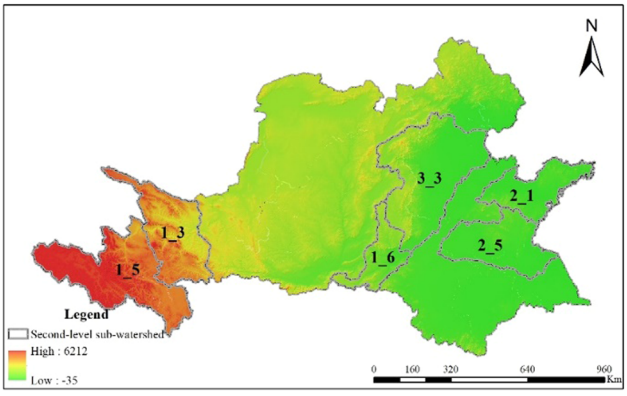

Figure 9: Areas with different land use space simulation results.

the lower the survival rate [45]. Drought reduces soil moisture content, and prolonged drought causes trees to die due to long-term lack of moisture [46]. The impact of repeated extreme precipitation events, such as repeated extreme drought events, even several years apart, may also have a greater negative impact on vegetation mortality [12]. As the North China Plain is strongly affected by the temperate monsoon, floods caused by heavy rains have had a huge negative impact on the Loess Plateau in the Yellow River Basin. More and more extreme precipitation has caused many environmental problems and ecological crises, such as soil erosion and land desertification [47]; for the Huai River Basin, since 1950, small floods have occurred every 2 years, and major floods have occurred every 5 years [48]; for the Haihe River Basin, although the annual precipitation is not large, most of the rainfall in the past 50 years has been reduced in the form of heavy rain, and the intensity of the heavy rain has been increasing [49]. In recent years, extreme hydrological events in all regions show an increasing trend. Floods mainly reduce vegetation through physical damage, and droughts reduce vegetation mainly through physiological damage. Based on the results of the net land-use change and exchange change and the land-use conversion matrix from 1980 to 2010, it is possible to know the conversion probability and direction of land use. Cultivated land, forest and grassland are frequently transformed into each other, while artificial surface is not easily transformed into other land types, and have strong expansion [50,51]. Under natural conditions, the probability of land use conversion is also one of the reasons for the difference in the spatial distribution of land use.

5.2 Impact of future climate on land use/cover

Compared with 2010, the spatial pattern of land use has changed in the future (Year 2030). We used the secondary watershed to make spatial statistics on the land-use pattern, and the results show that the distribution patterns of a forest, grassland, and cultivated land significantly change in the source and downstream region. The spatial distribution of areas with significant changes in the secondary watershed, shown in Figure 10. In the RCP 2.6 scenario, the area of cultivated land use in the upstream is reduced by more than 30%, while that is less than 10% in the RCP 4.5 and RCP 8.5 scenario. Whereas the area of grassland in downstream is reduced by more than 30% under the RCP 2.6 scenario but less than 10% under 10% under the RCP 4.5 and RCP 8.5 scenarios. According to the analysis of climatic conditions, the major factor for the different land-use patterns in upstream and downstream is precipitation. In the future, human activities will aim to minimize the disturbance of the natural environment and carry out green development [52]. Precipitation and temperature play the important roles in the growth of vegetation [53]. Therefore, precipitation and temperature will become the main factors affecting vegetation in the future. The risk of drought disaster risk in the Huang-Huai-Hai river basin is mainly reflected in the growing season precipitation in the entire region, the frequency of drought events, and the regulation and storage effect of the underlying surface on precipitation [54]. The higher risk areas are concentrated in the upper reaches of the basin. The risk of flood disaster risk in the Huang-Huai-Hai river basin is mainly reflected in the extreme precipitation in the entire basin and the regulation and storage effect of the underlying surface on

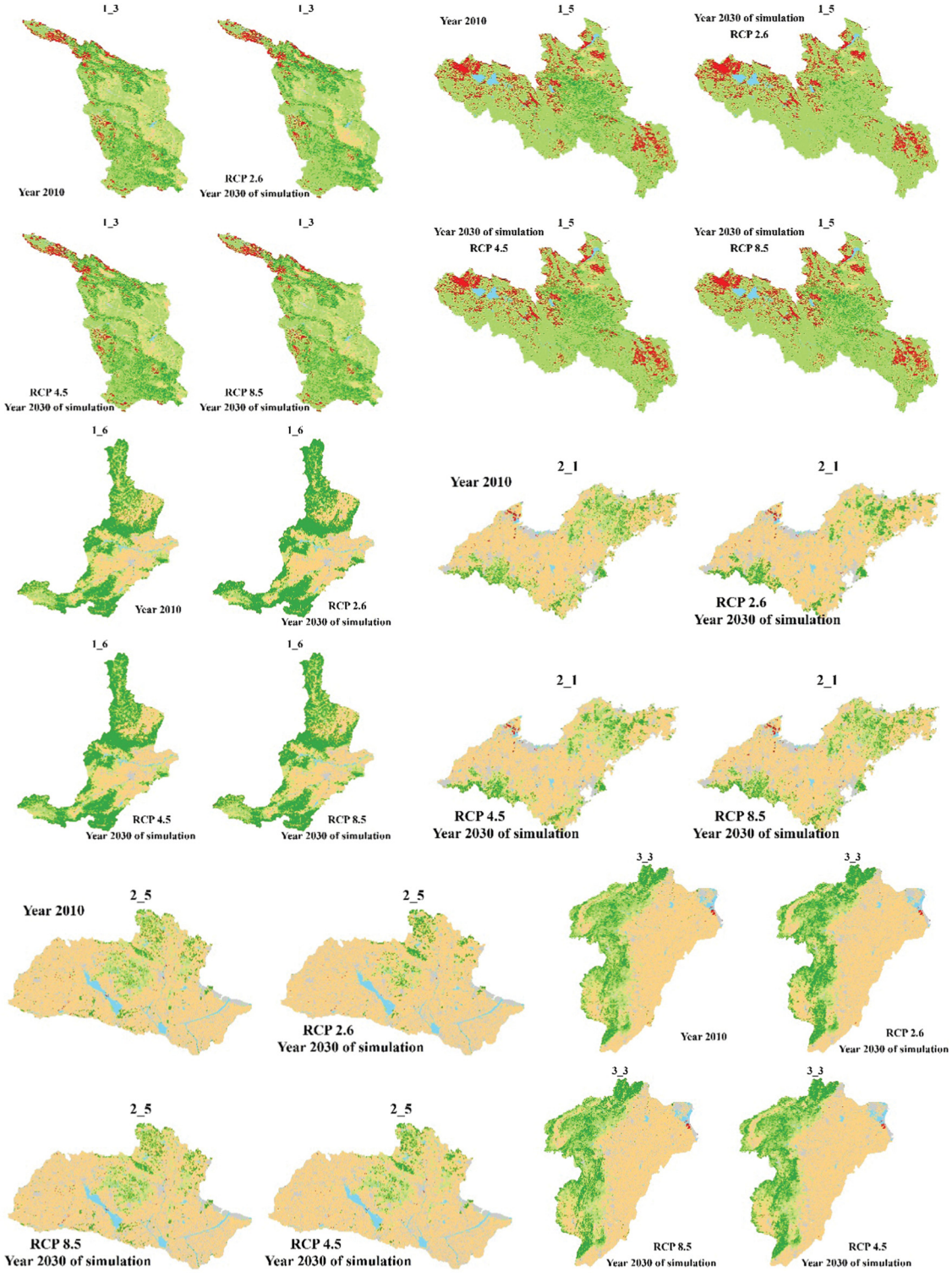

Figure 10: Areas with different land use spatial distribution in different climate condition.

precipitation [55]. The higher risk areas are concentrated in the lower reaches of the basin. The risk of drought and flood events in the basin in the future will have an impact on land use. At the same time, the pattern of land-use change in the upstream was different from that in the downstream. The upstream is dominated by the

Table 11: The meaning of the basin number

Basin number	Meaning
1_3	Catchment area from Longyangxia to Lanzhou
1_5	Catchment area above Longyangxia
1_6	Catchment area from Sanmenxia to Huayuankou
2_1	Catchment area of coastal rivers of Shangdong peninsula
2_5	Yishusi river basin
3_3	South of Haihe river basin

reduction of cultivated land, and the downstream is dominated by the reduction of grassland. That is because precipitation in the upstream will decrease 30 mm and that will increase about 40 mm in the downstream in the future. There is a large area of farmland upstream of the whole basin, which is affected not only by rainwater but also by artificial irrigation from the Yellow River. Therefore, with the participation of human activities, the area of cultivated land in the future may not be reduced much.

6 Conclusions

LUCC is affected by humans and climate change. By analyzing the historical changes in land use, the land-use changes after the 1990s had been dramatic, mainly reflected in the reduction of cultivated land and the expansion of artificial land. The social reason was mainly due to the increase in population, and the climatic reason was the increase in temperature. At the same time, this paper also studied the spatial distribution of land use in future climate scenarios. The changes in the upstream and downstream regions were the most obvious. The obvious changes in land use types were cultivated tland, grassland, and forest. The major factor was precipitation.

This article analyzes the causes of LUCC from the perspective of climatic conditions. The spatial distribution of land use in future climate conditions was also predicated. This result can also provide data support for future research on land use under future climate conditions.

Acknowledgments: This study was supported by the National Key Research and Development Project (Grant No. 2017YFA0605004; 2016YFA0601503) and the National Science Fund for Distinguished Young Scholars (Grant No. 51725905 and 51879275) and the National Natural Science Foundation of China (No. 51809002).

References

[1] Veldkamp A, Lambin EF. Predicting land-use change. Agric Ecosyst Environ. 2001;85(1):1–6. doi: 10.1016/S0167-8809(01)00199-2.

[2] Weinzettel J, Hertwich EG, Peters GP, Steen-Olsen K, Galli A. Affluence drives the global displacement of land use. Global Environ Change. 2013;23(2):433–8. doi: 10.1016/j.gloenvcha.2012.12.010.

[3] Jia K. Forest cover changes in the three-north shelter forest region of China during 1990 to 2005. J Environ Informat. 2015;26(2):126–37. doi: 10.3808/jei.201400268.

[4] Jamal M, Baba VV. Land-use and land-cover change. Science/research plan. Global Change Rep. 1995;43:669–79. doi: 10.1177/001872679104401105.

[5] Lambin EF, Turner BL, Geist HJ, Agbola SB, Angelsen A, Bruce JW, et al. The causes of land-use and land-cover change: moving beyond the myths. Global Environ Change. 2001;11(4):261–9. doi: 10.1016/S0959-3780(01)00007-3.

[6] Seeber C, Hartmann H, Xiang W, King L. Land use change and causes in the Xiangxi catchment, three Gorges area derived from multispectral data. J Earth Sci, 2010;21(6):846–55. doi: 10.1007/s12583-010-0136-7.

[7] van Vliet J, de Groot HLF, Rietveld P, Verburg PH. Manifestations and underlying drivers of agricultural land use change in Europe. Landscape Urban Plan, 2015;133:24–36. doi: 10.1016/j.landurbplan.2014.09.001.

[8] Long H, Tang G, Li X, Heilig GK. Socio-economic driving forces of land-use change in Kunshan, the Yangtze River Delta economic area of China. J Environ Manage, 2007;83(3):351–64. doi: 10.1016/j.jenvman.2006.04.003.

[9] Long HL, Li XB. Rural housing land transition in transect of the Yangtze River [in Chinese with English abstract]. Acta Geograph Sin. 2005;60:179–88. doi: 10.3321/j.issn:0375-5444.2005.02.001.

[10] Vadrevu K, Heinimann A, Gutman G, Justice C. Remote sensing of land use/cover changes in South and Southeast Asian Countries. Int J Dig Earth. 2019;12(10):1099–102. doi: 10.1080/17538947.2019.1654274.

[11] Xu HJ, Wang XP, Zhang XX. Decreased vegetation growth in response to summer drought in Central Asia from 2000 to 2012. Int J Appl Earth Observ Geoinform. 2016;52:390–402. doi: 10.1016/j.jag.2016.07.010.

[12] Anderegg WRL, Plavcová L, Anderegg LDL, Hacke UG, Berry JA, Field CB. Drought's legacy: multiyear hydraulic deterioration underlies widespread aspen forest die-off and portends increased future risk. Global Change Biol. 2013;19(4):1188–96. doi: 10.1111/gcb.12100.

[13] Ibáñez B, Gómez-Aparicio L, Stoll P, Ávila JM, Pérez-Ramos IM, Marañón T. A neighborhood analysis of the consequences of

Quercus suber decline for regeneration dynamics in Mediterranean forests. PLoS One. 2015;10(2):1–18. doi: 10.1371/journal.pone.0117827.
[14] Arowolo AO, Deng X. Land use/land cover change and statistical modelling of cultivated land change drivers in Nigeria. Region Environ Change. 2018;18(1):247–59. doi: 10.1007/s10113-017-1186-5.
[15] Reis S. Analyzing land use/land cover changes using remote sensing and GIS in Rize, North-East Turkey. Sensors. 2008;8(10):6188–202. doi: 10.3390/s8106188.
[16] Chen J, Gong P, He C, Pu R, Shi P. Land-use/land-cover change detection using improved change-vector analysis. Photogramm Eng Remote Sens. 2003;69(4):369–79. doi: 10.14358/PERS.69.4.369.
[17] Yu W, Zang S, Wu C, Liu W, Na X. Analyzing and modeling land use land cover change (LUCC) in the Daqing City, China. Appl Geograph. 2011;31(2):600–8. doi: 10.1016/j.apgeog.2010.11.019.
[18] Cao J, Wu J, Li C. The forecast of land use and land cover change tendency based on Markov process in Suzhou District Jiuquan City Gansu Province [in Chinese with English abstract]. Territory Nat Resour Study. 2008;1:45–7.
[19] Yulianto F, Maulana T, Khomarudin MR. Analysis of the dynamics of land use change and its prediction based on the integration of remotely sensed data and CA-Markov model, in the upstream Citarum Watershed, West Java, Indonesia. Int J Dig Earth. 2019;12(10):1151–76. doi: 10.1080/17538947.2018.1497098.
[20] Verburg PH, Soepboer W, Veldkamp A, Limpiada R, Espaldon V, Mastura SSA. Modeling the spatial dynamics of regional land use: The CLUE-S model. Environ Manage. 2003;30(3):391–405. doi: 10.1007/s00267-002-2630-x.
[21] Verburg PH, Overmars KP. Combining top-down and bottom-up dynamics in land use modeling: exploring the future of abandoned farmlands in Europe with the Dyna-CLUE model. Landscape Ecol. 2009;24(9):1167–81. doi: 10.1007/s10980-009-9355-7.
[22] Liu X, Liang X, Li X, Xu X, Ou J, Chen Y, et al. A future land use simulation model (FLUS) for simulating multiple land use scenarios by coupling human and natural effects. Landscape Urban Plan. 2017;168:94–116. doi: 10.1016/j.landurbplan.2017.09.019.
[23] Pancost RD. Cities lead on climate change. Nat Geosci. 2016;9(4):264–6. doi: 10.1038/ngeo2690.
[24] Lu D, Mausel P, Brondízio E, Moran E. Change detection techniques. Int J Remote Sens. 2004;25(12):2365–401. doi: 10.1080/0143116031000139863.
[25] Shen F, Geng L, Qin F, Xu P. Analysis of water saving in received area in Huang-Huai-Hai watersheds and Eastern and Middle Lines of Water Transferring Project from South to North, China [in Chinese with English abstract]. Adv Water Sci. 2002;13(6):768–74.
[26] Liu M, Wu J, Lv A, Zhao L, He B. The water stress of winter wheat in Huang-Huai-Hai Plain of China under rain-fed condition [in Chinese with English abstract]. Progr Geograph. 2010;29(4):427–32. doi: 10.11820/dlkxjz.2010.04.006.
[27] National Standards of the People's Republic of China (GBT_21010_2017). Current and use classification, Beijing, Standards Press of China, 2017. (in Chinese with English abstract).
[28] Huang C, Teng M, Zeng L, Zhou Z, Xiao W, Zhu J, et al. Long-term changes of land use/cover in the Three Gorges Reservoir Area of the Yangtze River, China [in Chinese with English abstract]. J Appl Ecol. 2018;29(05):1585–96.
[29] Yang X, Zheng X, Chen R. A land use change model: integrating landscape pattern indexes and Markov-CA. Ecol Modell. 2014;283:1–7. doi: 10.1016/j.ecolmodel.2014.03.011.
[30] Zhang R, Tang C, Ma S, Yuan H, Gao L, Fan W. Using Markov chains to analyze changes in wetland trends in arid Yinchuan Plain, China. Math Comput Modell. 2011;54(3–4):924–30. doi: 10.1016/j.mcm.2010.11.017.
[31] Prestele R, Alexander P, Rounsevell MDA, Arneth A, Calvin K, Doelman J, et al. Hotspots of uncertainty in land-use and land-cover change projections: a global-scale model comparison. Global Change Biol. 2016;22(12):3967–83. doi: 10.1111/gcb.13337.
[32] Mondal MS, Sharma N, Garg PK, Kappas M. Statistical independence test and validation of CA Markov land use land cover (LULC) prediction results. Egyptian J Remote Sens Space Sci. 2016;19(2):259–72. doi: 10.1016/j.ejrs.2016.08.001.
[33] Zheng HW, Shen GQ, Wang H, Hong J. Simulating land use change in urban renewal areas: a case study in Hong Kong. Habitat Int, 2015;46:23–34. doi: 10.1016/j.habitatint.2014.10.008.
[34] Overmars KP, Koning DGHJ. Spatial autocorrelation in multi-scale land use models. Ecol Modell. 2003;164:257–70. doi: 10.1016/S0304-3800(03)00070-X.
[35] Dan W, Wei H, Shuwen Z, Kun B, Bao X, Yi W, et al. Processes and prediction of land use/land cover changes (LUCC) driven by farm construction: the case of Naoli River Basin in Sanjiang Plain. Environ Earth Sci. 2015;73(8):4841–51. doi: 10.1007/s12665-014-3765-9.
[36] Verburg PH, Rounsevell MDA, Veldkamp A. Scenario-based studies of future land use in Europe. Agric Ecosyst Environ. 2006;114(1):1–6. doi: 10.1016/j.agee.2005.11.023.
[37] Guan D, Li H, Inohae T, Su W, Nagaie T, Hokao K. Modeling urban land use change by the integration of cellular automaton and Markov model. Ecol Modell. 2011;222(20):3761–72. doi: 10.1016/j.ecolmodel.2011.09.009.
[38] Li X, Chen G, Liu X, Liang X, Wang S, Chen Y, et al. A new global land-use and land-cover change product at a 1-km resolution for 2010 to 2100 based on human-environment interactions. Anna Am Assoc Geograph. 2017;107(5):1040–59. doi: 10.1080/24694452.2017.1303357.
[39] Pencina M, D'agostino RBJ, Vasan R. Evaluating the added predictive ability of a new marker: From area under the ROC curve to reclassification and beyond. Stat Med. 2008;27(2):112–57. doi: 10.1002/sim.2929.
[40] Kyakuno T. Prediction of land use changes with Bayesian spatial modeling from the perspective of urban climate. Urban Climate. 2020;31:100569. doi: 10.1016/j.uclim.2019.100569.
[41] Pontius RG, Boersma W, Castella JC, Clarke K, de Nijs T, Dietzel C, et al. Comparing the input, output, and validation maps for several models of land change. Ann Region Sci. 2008;42(1):11–37. doi: 10.1007/s00168-007-0138-2.
[42] Wu X, Liu H, Li X, Ciais P, Babst F, Guo W, et al. Differentiating drought legacy effects on vegetation growth over the temperate northern hemisphere. Glob Chang Biol. 2017;24(1):504–16. doi: 10.1111/gcb.13920.

[43] Zeppel MJB, Wilks JV, Lewis JD. Impacts of extreme precipitation and seasonal changes in precipitation on plants. Biogeoences. 2014;11:3083–93. doi: 10.5194/bg-11-3083-2014.
[44] Matusick G, Ruthrof KX, Kala J, Brouwers NC, Breshears DD, Hardy GESJ. Chronic historical drought legacy exacerbates tree mortality and crown dieback during acute heat-wave-compounded drought. Environ Res Lett. 2018;13(9):1–14. doi: 10.1088/1748-9326/aad8cb.
[45] Tzeng HY, Wang W, Tseng YH, Chiu CA, Tsai ST. Tree mortality in response to typhoon-induced floods and mudslides is determined by tree species, size, and position in a riparian formosan gum forest in subtropical taiwan. PLoS One. 2018;13(1):e0190832. doi: 10.1371/journal.pone.0190832.
[46] Harper CW, Blair JM, Fay PA, Knapp AK, Carlisle JD. Increased rainfall variability and reduced rainfall amount decreases soil co2 flux in a grassland ecosystem. Global Change Biol. 2005;11(2):322–34. doi: 10.1111/j.1365-2486.2005.00899.x.
[47] He Z, He J. Temporal and spatial variation of extreme precipitation in the Yellow River Basin from 1960 to 2012 [in Chinese with English abstract]. Resour Sci. 2014;36(3):490–501.
[48] She D, Xia J, Zhang Y, Du H. The trend analysis and statistical distribution of extreme rainfall events in the Huaihe River Basin in the past 50 years [in Chinese with English abstract]. Acta Geograph Sin. 2011;66(9):1200–10.
[49] Pei Y, Wang J, Luo L. Analysis of effect of South-to-North Water Transfer Project on aquatic ecosystems of Haihe River Basin [in Chinese with English abstract]. Acta Ecol Sin. 2004;24(10):2115–23.
[50] Pontius RG, Millones M. Death to Kappa: birth of quantity disagreement and allocation disagreement for accuracy assessment. Int J Remote Sens. 2011;32(15):4407–29. doi: 10.1080/01431161.2011.552923.
[51] Piani C, Weedon GP, Best M, Gomes SM, Viterbo P, Hagemann S, et al. Statistical bias correction of global simulated daily precipitation and temperature for the application of hydrological models. J Hydrol. 2010;395(3–4):199–215. doi: 10.1016/j.jhydrol.2010.10.024.
[52] Jung SH, Feng T. Government subsidies for green technology development under uncertainty. Eur J Operat Res. 2020;286(2):726–39. doi: 10.1016/j.ejor.2020.03.047.
[53] Li W, Du J, Li S, Zhou X, Duan Z, Li R, et al. The variation of vegetation productivity and its relationship to temperature and precipitation based on the GLASS-LAI of different African ecosystems from 1982 to 2013. Int J Biometeorol 2019;63(7):847–60. doi: 10.1007/s00484-019-01698-x.
[54] Wilby RL. Greenhouse hydrology. Progr Phys Geograph. 1995;19(3):351–69. doi: 10.1177/030913339501900304.
[55] Gázquez F, Calaforra JM, Fernández-Cortés Á. Flash flood events recorded by air temperature changes in caves: a case study in Covadura Cave (SE Spain). J Hydrol. 2016;541:136–45. doi: 10.1016/j.jhydrol.2015.10.059.